

Magnon Exchange Mechanism of Ferromagnetic Superconductivity

Naoum Karchev*

Department of Physics, University of Sofia, 1126 Sofia, Bulgaria

The magnon exchange mechanism of ferromagnetic superconductivity (FM-superconductivity) was developed to explain in a natural way the fact that the superconductivity in UGe_2 , $ZrZn_2$ and $URhGe$ is confined to the ferromagnetic phase. The order parameter is a spin anti-parallel component of a spin-1 triplet with zero spin projection. The transverse spin fluctuations are pair forming and the longitudinal ones are pair breaking. In the present paper, a superconducting solution, based on the magnon exchange mechanism, is obtained which closely matches the experiments with $ZrZn_2$ and $URhGe$. The onset of superconductivity leads to the appearance of complicated Fermi surfaces in the spin up and spin down momentum distribution functions. Each of them consist of two pieces, but they are simple-connected and can be made very small by varying the microscopic parameters. As a result, it is obtained that the specific heat depends on the temperature linearly, at low temperature, and the coefficient $\gamma = \frac{C}{T}$ is smaller in the superconducting phase than in the ferromagnetic one. The absence of a quantum transition from ferromagnetism to ferromagnetic superconductivity in a weak ferromagnets $ZrZn_2$ and $URhGe$ is explained accounting for the contribution of magnon self-interaction to the spin fluctuations' parameters. It is shown that in the presence of an external magnetic field the system undergoes a first order quantum phase transition.

74.20.Mn, 75.50.Cc, 75.10.Lp

I Introduction

Very recently ferromagnetic superconductivity (FM-superconductivity) has been observed in UGe_2 [1], $ZrZn_2$ [2] and $URhGe$ [3]. The superconductivity is confined to the ferromagnetic phase. Ferromagnetism and superconductivity are believed to arise due to the same band electrons. The persistence of ferromagnetic order within the superconducting phase has been ascertained by neutron scattering. The specific heat anomaly associated with the superconducting transition in these materials appears to be absent.

At ambient pressure UGe_2 is an itinerant ferromagnet below the Curie temperature $T_c = 52K$, with low-temperature ordered moment of $\mu_s = 1.4\mu_B/U$. With increasing pressure the system passes through two successive quantum phase transition, from ferromagnetism to FM-superconductivity at $P \sim 10$ kbar, and at higher pressure $P_c \sim 16$ kbar to paramagnetism [1,4]. At the pressure where the superconducting transition temperature is a maximum $T_{sc} = 0.8K$, the ferromagnetic state is still stable with $T_c = 32K$, and the system undergoes

a first order metamagnetic transition between two ferromagnetic phases with different ordered moments [5]. The specific heat coefficient $\gamma = \frac{C}{T}$ increases steeply near 11 kbar and retains a large and nearly constant value [6].

The ferromagnets $ZrZn_2$ and $URhGe$ are superconducting at ambient pressure with superconducting critical temperatures $T_{sc} = 0.29K$ and $T_{sc} = 0.25K$ respectively. $ZrZn_2$ is ferromagnetic below the Curie temperature $T_c = 28.5K$ with low-temperature ordered moment of $\mu_s = 0.17\mu_B$ per formula unit, while for $URhGe$ $T_c = 9.5K$ and $\mu_s = 0.42\mu_B$. The low Curie temperatures and small ordered moments indicate that compounds are close to a ferromagnetic quantum critical point. A large jump in the specific heat, at the temperature where the resistivity becomes zero, is observed in $URhGe$. At low temperature the specific heat coefficient γ is twice smaller than in the ferromagnetic phase. materials

The most popular theory of FM-superconductivity is based on the paramagnon exchange mechanism [7,8]. The order parameters are spin parallel components of the spin triplet. The superconductivity in $ZrZn_2$ was predicted, but the theory meets many difficulties. In order to explain the absence of superconductivity in paramagnetic phase it was accounted for the magnon paramagnon interaction and proved that the critical temperature is much higher in the ferromagnetic phase than in the paramagnetic one [9]. To the same purpose, the Ginzburg-Landau mean-field theory was modified with an exchange-type interaction between the magnetic moments of triplet-state Cooper pairs and the ferromagnetic magnetization density [10].

The Fay and Appel (FA) theory predicts that spin up and spin down fermions form Cooper pairs, and hence the specific heat decreases exponentially at low temperature. The phenomenological theories [11] circumvent the problem assuming that only majority spin fermions form pairs, and hence the minority spin fermions contribute the asymptotic of the specific heat. The coefficient $\gamma = \frac{C}{T}$ is twice smaller in the superconducting phase, which closely matches the experiments with $URhGe$ [3] but does not resemble the experimental results for UGe_2 and $ZrZn_2$. The assumption seems to be doubtful for systems with very small ordered moment.

The superconducting critical temperature in (FA) theory increases when the magnetization decreases and very close to the quantum critical point falls down rapidly. It has recently been the subject of controversial debate. It is obtained in [12], by means of a more complete Eliashberg treatment, that the transition temperature is nonzero at the critical point. In [13], however, the authors have

shown that the reduction of quasiparticle coherence and life-time due to spin fluctuations is the pair-breaking process which leads to a rapid reduction of the superconducting critical temperature near the quantum critical point.

Recent studies of polycrystalline samples of UGe_2 show that T-P phase diagram is very similar to those of single-crystal specimens of UGe_2 [14]. These findings suggest that the superconductivity in UGe_2 is relatively insensitive to the presence of impurities and defects which excludes the spin parallel pairing.

Despite of the efforts, the improved theory of paramagnon induced superconductivity can not cover the whole variety of properties of FM-superconductivity.

Magnon exchange mechanism of superconductivity has been proposed [15] to explain in a natural way the fact that the superconductivity in UGe_2 , $ZrZn_2$ and $URhGe$ is confined to the ferromagnetic phase. The order parameter is a spin anti-parallel component $\uparrow\downarrow + \downarrow\uparrow$ of a spin-1 triplet ($\uparrow\uparrow, \uparrow\downarrow + \downarrow\uparrow, \downarrow\downarrow$) with zero spin projection. The transverse spin fluctuations are pair forming and the longitudinal ones are pair breaking. The competition between magnons and paramagnons explains the existence of the two successive quantum phase transitions in UGe_2 .

An itinerant system is considered in which the spin- $\frac{1}{2}$ fermions responsible for the ferromagnetism are the same quasiparticles which form the Cooper pairs. Hence, one has to consider the equation for the gap as well as the equation for the magnetization. Then the system of equations for the gap and for the magnetization determines the phase where the superconductivity and the ferromagnetism coexist.

In the present paper, a superconducting solution, based on the magnon exchange mechanism, is obtained which closely matches the experiments with $ZrZn_2$ and $URhGe$. The proposed superconducting solution differs from the superconducting solution discussed in [15] in two ways. First, the quantum phase transition from ferromagnetism to FM-superconductivity is smooth second order phase transition, which resembles the experimental results for UGe_2 . In the present paper, the system passes through a first order quantum phase transition. Second, to form a Cooper pair an electron transfers from one Fermi surface to the other. As a result, the onset of superconductivity in [15] leads to the appearance of two Fermi surfaces in each of the spin up and spin down momentum distribution functions. The existence of the two Fermi surfaces explains the linear dependence of the specific heat at low temperatures as opposed to the exponential decrease of the specific heat in the BCS theory. In the ferromagnetic phase the specific heat constant γ is smaller than in the superconducting one, which closely matches the experiments with UGe_2 [6]. The onset of superconductivity, in the present paper, leads to the appearance of complicated Fermi surfaces in the spin up and spin down momentum distribution functions. Each of them consist of two pieces, but they are simple-connected and can be made very small by varying the microscopic parameters. As a result, $\gamma = \frac{C}{T}$ can be made smaller in

FM-superconducting phase in agreement with $URhGe$ experiments [3].

The existence of two Fermi surfaces in each of the spin-up and spin-down momentum distribution functions is a generic property of a FM-superconductivity with spin anti-parallel pairing. An important example is the coexistence of ferromagnetism and s-superconductivity induced by phonons [16]. The spin fluctuations are pair breaking if the order parameter is spin singlet [17], and superconductivity and ferromagnetism coexist if the spin fluctuations are weak, while the magnon-induced superconductivity coexist with ferromagnetism close to quantum critical point where the spin fluctuations are very strong. The present paper and [16] describe different physical realities which lead to coexistence of ferromagnetism and superconductivity.

The paper is organized as follows. In Sec.II an effective Hamiltonian is obtained. In Sec III, the magnon-induced superconductivity is discussed. The superconducting solution known from [15] is reported to complete the investigation. Section IV is devoted to the concluding remarks.

II Effective Hamiltonian

An itinerant system is considered in which the spin- $\frac{1}{2}$ fermions responsible for the ferromagnetism are the same quasiparticles which form the Cooper pairs. The effective interaction of quasiparticles $c_\sigma(\vec{x})(c_\sigma^\dagger(\vec{x}))$ with spin fluctuations has the form

$$H_{s-f} = J \int d^3x c^+(\vec{x}) \frac{\vec{\tau}}{2} c(\vec{x}) \cdot \vec{M}(\vec{x}) \quad (1)$$

where the transverse spin fluctuations are described by magnons

$$\begin{aligned} M_1(\vec{x}) + iM_2(\vec{x}) &= \sqrt{2M}a(\vec{x}), \\ M_1(\vec{x}) - iM_2(\vec{x}) &= \sqrt{2M}a^+(\vec{x}) \end{aligned} \quad (2)$$

and the longitudinal spin fluctuations by paramagnons

$$M_3(\vec{x}) - M = \varphi(\vec{x}). \quad (3)$$

M is zero temperature dimensionless magnetization of the system per lattice site.

The partition function can be written as a path integral over the complex functions of the Matsubara time τ $a(\tau, \vec{x}), a^+(\tau, \vec{x}), \varphi(\tau, \vec{x})$ and Grassmann functions $c_\sigma(\tau, \vec{x}), c_\sigma^\dagger(\tau, \vec{x})$ [18]

$$\mathcal{Z}(\beta) = \int D\mu (a^+, a, \varphi, c_\sigma^+, c_\sigma) e^{-S}. \quad (4)$$

The action is a sum of free action S_0 and part which describes the spin-fermion interaction S_{int} .

$$S_0 = \int_0^\beta d\tau \int \frac{d^3k}{(2\pi)^3} \left[a^+(\tau, \vec{k}) \dot{a}(\tau, \vec{k}) + \omega(\vec{k}) a^+(\tau, \vec{k}) a(\tau, \vec{k}) \right. \\ \left. + \varphi(\tau, \vec{k}) D_{pm}^{-1}(\tau, \vec{k}) \varphi(\tau, -\vec{k}) \right. \\ \left. + c_\sigma^+(\tau, \vec{k}) \dot{c}_\sigma(\tau, \vec{k}) + \epsilon_\sigma(\vec{k}) c_\sigma^+(\tau, \vec{k}) c_\sigma(\tau, \vec{k}) \right] \quad (5)$$

where β is the inverse temperature. The magnon's dispersion is

$$\omega(\vec{k}) = \rho \vec{k}^2 \quad (6)$$

where the spin stiffness constant is proportional to M ($\rho = M\rho_0$). The paramagnon propagator in Matsubara representation is

$$D_{pm}(\tau, \vec{k}) = \int \frac{d\omega}{(2\pi)} \frac{e^{i\omega\tau}}{r + \frac{|\omega|}{|\vec{k}|} + b\vec{k}^2}. \quad (7)$$

The parameter r is the inverse static longitudinal magnetic susceptibility, which measures the deviation from quantum critical point. The constants J, ρ_0 and b are phenomenological ones subject to some relations. Finally, the spin-up and spin-down fermions have the following dispersion relations:

$$\epsilon_\uparrow(\vec{k}) = \frac{\vec{k}^2}{2m} - \mu - \frac{JM}{2}, \quad \epsilon_\downarrow(\vec{k}) = \frac{\vec{k}^2}{2m} - \mu + \frac{JM}{2} \quad (8)$$

Accounting for Eqs(2) and (3) one obtains the following expression for the interacting part of the action

$$S_{\text{int}} = \frac{J}{2} \int_0^\beta d\tau \int d^3x \left[\sqrt{2M} c_\uparrow^+(\tau, \vec{x}) c_\downarrow(\tau, \vec{x}) a(\tau, \vec{x}) \right. \\ \left. + \sqrt{2M} c_\downarrow^+(\tau, \vec{x}) c_\uparrow(\tau, \vec{x}) a^+(\tau, \vec{x}) \right. \\ \left. + \left(c_\uparrow^+(\tau, \vec{x}) c_\uparrow(\tau, \vec{x}) - c_\downarrow^+(\tau, \vec{x}) c_\downarrow(\tau, \vec{x}) \right) \varphi(\tau, \vec{x}) \right] \quad (9)$$

The integral Eq.(4) over the bose fields (a, a^+, φ) is Gaussian. Integrating them out, using the formula for the Gaussian integral [18], one obtains a representation for the partition function in terms of path integral over the Grassmann fields.

$$\mathcal{Z}(\beta) = \int D\mu(c^+, c) e^{-S_{eff}}. \quad (10)$$

The effective fermion action S_{eff} is a sum of free part and resulting four-fermion interaction S_{f4}

$$S_{f4} = -\frac{J^2}{8} \int d^4x_1 d^4x_2 \left[c_\uparrow^+(x_1) c_\uparrow(x_1) - c_\downarrow^+(x_1) c_\downarrow(x_1) \right] \\ D_{pm}(x_1 - x_2) \left[c_\uparrow^+(x_2) c_\uparrow(x_2) - c_\downarrow^+(x_2) c_\downarrow(x_2) \right] - \quad (11) \\ \frac{MJ^2}{2} \int d^4x_1 d^4x_2 c_\downarrow^+(x_1) c_\uparrow(x_1) D_m(x_1 - x_2) c_\uparrow^+(x_2) c_\downarrow(x_2).$$

where $x = (\tau, \vec{x})$, D_{pm} is the paramagnon propagator Eq.(7), and D_m is the magnon Green function

$$D_m(x) = \int \frac{d\omega}{2\pi} \frac{d^3k}{(2\pi)^3} \frac{e^{-i\omega\tau + i\vec{k}\vec{x}}}{i\omega + \rho\vec{k}^2} \quad (12)$$

For the purpose of doing analytical calculations it is convenient to approximate the four-fermion interaction with the static one. To this end I replace the magnon and paramagnon propagators Eqs.(12,7) by static potentials

$$2M D_m(\omega, \vec{k}) \rightarrow V_m(\vec{k}) = \frac{2M}{\rho\vec{k}^2} \quad (13)$$

$$D_{pm}(\omega, \vec{k}) \rightarrow V_{pm}(\vec{k}) = \frac{1}{r + b\vec{k}^2}.$$

The next step is to represent the spin anti-parallel composite field $c_\uparrow c_\downarrow$ as a sum of symmetric and antisymmetric parts. After some algebra one obtains an effective four fermion theory which can be written as a sum of four terms. Three of them describe the interaction of the components of spin-1 composite fields ($\uparrow\uparrow, \uparrow\downarrow + \downarrow\uparrow, \downarrow\downarrow$) which have a projection of spin 1,0 and -1 respectively. The fourth term describes the interaction of the spin singlet composite fields $\uparrow\downarrow - \downarrow\uparrow$. The Hamiltonians of interactions are

$$H_{\uparrow\uparrow} = -\frac{J^2}{8} \int \prod_i \frac{d^3k_i}{(2\pi)^3} \left[c_\uparrow^+(\vec{k}_1) c_\uparrow^+(\vec{k}_2) \right. \\ \left. c_\uparrow(\vec{k}_2 - \vec{k}_3) c_\uparrow(\vec{k}_1 + \vec{k}_3) \right] V_{pm}(\vec{k}_3) \quad (14)$$

$$H_{\downarrow\downarrow} = -\frac{J^2}{8} \int \prod_i \frac{d^3k_i}{(2\pi)^3} \left[c_\downarrow^+(\vec{k}_1) c_\downarrow^+(\vec{k}_2) \right. \\ \left. c_\downarrow(\vec{k}_2 - \vec{k}_3) c_\downarrow(\vec{k}_1 + \vec{k}_3) \right] V_{pm}(\vec{k}_3) \quad (15)$$

$$H_p = -\frac{J^2}{8} \int \prod_i \frac{d^3k_i}{(2\pi)^3} \left[c_\uparrow^+(\vec{k}_1) c_\downarrow^+(\vec{k}_2) + c_\downarrow^+(\vec{k}_1) c_\uparrow^+(\vec{k}_2) \right] \quad (16)$$

$$\left[c_\uparrow(\vec{k}_2 - \vec{k}_3) c_\downarrow(\vec{k}_1 + \vec{k}_3) + c_\downarrow(\vec{k}_2 - \vec{k}_3) c_\uparrow(\vec{k}_1 + \vec{k}_3) \right] V_-(\vec{k}_3)$$

$$H_s = \frac{J^2}{16} \int \prod_i \frac{d^3k_i}{(2\pi)^3} \left[c_\uparrow^+(\vec{k}_1) c_\downarrow^+(\vec{k}_2) - c_\downarrow^+(\vec{k}_1) c_\uparrow^+(\vec{k}_2) \right] \quad (17)$$

$$\left[c_\uparrow(\vec{k}_2 - \vec{k}_3) c_\downarrow(\vec{k}_1 + \vec{k}_3) - c_\downarrow(\vec{k}_2 - \vec{k}_3) c_\uparrow(\vec{k}_1 + \vec{k}_3) \right] V_+(\vec{k}_3)$$

where

$$V_-(\vec{k}) = \frac{2M}{\rho\vec{k}^2} - \frac{1}{r + b\vec{k}^2}, \quad V_+(\vec{k}) = \frac{2M}{\rho\vec{k}^2} + \frac{1}{r + b\vec{k}^2} \quad (18)$$

The spin singlet fields' interaction Eq.(17) is repulsive and does not contribute to the superconductivity [17]. The spin parallel fields' interactions Eqs.(14,15) are due to the exchange of paramagnons and do not contribute to the magnon-mediated superconductivity. The relevant interaction is that of the $\uparrow\downarrow + \downarrow\uparrow$ fields Eq.(16). It has an attracting part due to exchange of magnons and a repulsive part due to exchange of paramagnons.

The effective Hamiltonian of the system is

$$H_{eff} = H_0 + H_p \quad (19)$$

where H_0 is the Hamiltonian of the free spin up and spin down fermions with dispersions Eq.(8).

III Magnon-Induced Superconductivity

By means of the Hubbard-Stratanovich transformation one introduces $\uparrow\downarrow + \downarrow\uparrow$ composite field and then the fermions can be integrated out. The obtained free energy is a function of the composite field and the integral over the composite field can be performed approximately by means of the steepest descend method. To this end one sets the first derivative of the free energy with respect to composite field equal to zero, this is the gap equation. To ensure that the fermions which form Cooper pairs are the same as those responsible for spontaneous magnetization, one has to consider the equation for the magnetization as well.

$$M = \frac{1}{2} \langle c_{\uparrow}^{\dagger} c_{\uparrow} - c_{\downarrow}^{\dagger} c_{\downarrow} \rangle \quad (20)$$

The system of equations for the gap and for the magnetization determines the phase where the superconductivity and the ferromagnetism coexist.

The system can be written in terms of Bogoliubov excitations, which have the following dispersions relations:

$$\begin{aligned} E_1(\vec{k}) &= -\frac{JM}{2} - \sqrt{\epsilon^2(\vec{k}) + |\Delta(\vec{k})|^2} \\ E_2(\vec{k}) &= \frac{JM}{2} - \sqrt{\epsilon^2(\vec{k}) + |\Delta(\vec{k})|^2} \end{aligned} \quad (21)$$

where $\Delta(\vec{k})$ is the gap, and $\epsilon(\vec{k}) = \frac{\vec{k}^2}{2m} - \mu$. At zero temperature the equations take the form

$$M = \frac{1}{2} \int \frac{d^3k}{(2\pi)^3} [1 - \Theta(-E_2(\vec{k}))] \quad (22)$$

$$\Delta(\vec{p}) = \frac{J^2}{8} \int \frac{d^3k}{(2\pi)^3} \frac{V(\vec{p} - \vec{k}) \Theta(-E_2(\vec{k}))}{\sqrt{\epsilon^2(\vec{k}) + |\Delta(\vec{k})|^2}} \Delta(\vec{k}) \quad (23)$$

The gap is an antisymmetric function $\Delta(-\vec{k}) = -\Delta(\vec{k})$, so that the expansion in terms of spherical harmonics $Y_{lm}(\Omega_{\vec{k}})$ contains only terms with odd l . I assume that the component with $l = 1$ and $m = 0$ is nonzero and the other ones are zero

$$\Delta(\vec{k}) = \Delta_{10}(k) \sqrt{\frac{3}{4\pi}} \cos \theta. \quad (24)$$

Expanding the potential $V_-(k)$ in terms of Legendre polynomial P_l one obtains that only the component with $l = 1$ contributes the gap equation. The potential $V_1(p, k)$ has the form,

$$\begin{aligned} V_1(p, k) &= \frac{3M}{\rho} \left[\frac{p^2 + k^2}{4p^2k^2} \ln \left(\frac{p+k}{p-k} \right)^2 - \frac{1}{pk} \right] - \\ &\frac{3M}{\rho} \beta \left[\frac{p^2 + k^2}{4p^2k^2} \ln \frac{r' + (p+k)^2}{r' + (p-k)^2} - \frac{1}{pk} \right], \end{aligned} \quad (25)$$

where $\frac{3M}{\rho} = \frac{3}{\rho_0}$, $\beta = \frac{\rho}{2Mb} = \frac{\rho_0}{2b} > 1$ and $r' = \frac{\tau}{b} \ll 1$. A straightforward analysis shows that for a fixed p , the potential is positive when k runs an interval around p ($p - \Lambda, p + \Lambda$), where Λ is approximately independent on p . In order to allow for an explicit analytic solution, I introduce further simplifying assumptions by neglecting the dependence of $\Delta_{10}(k)$ on k ($\Delta_{10}(k) = \Delta_{10}(p_f) = \Delta$) and setting $V_1(p_f, k)$ equal to a constant V_1 within interval $(p_f - \Lambda, p_f + \Lambda)$ and zero elsewhere. The system of equations (22,23) is then reduced to the system

$$M = \frac{1}{8\pi^2} \int_0^{\infty} dk k^2 \int_{-1}^1 dt [1 - \Theta(-E_2(k, t))] \quad (26)$$

$$\Delta = \frac{J^2 V_1}{32\pi^2} \int_{p_f - \Lambda}^{p_f + \Lambda} dk k^2 \int_{-1}^1 dt t^2 \frac{\Theta(-E_2(k, t))}{\sqrt{\epsilon^2(k) + \frac{3}{4\pi} t^2 \Delta^2}} \Delta \quad (27)$$

where $t = \cos \theta$.

III.1 Solution which satisfies $\sqrt{\frac{3}{\pi}} \Delta < JM$

The equation of magnetization (26) shows that it is convenient to represent the gap in the form $\Delta = \sqrt{\frac{\pi}{3}} \kappa(M) JM$, where $\kappa(M) < 1$. Then the equation

$$E_2(k, t) = 0, \quad (28)$$

defines the Fermi surfaces,

$$p_f^{\pm} = \sqrt{p_f^2 \pm m \sqrt{J^2 M^2 - \frac{3}{\pi} t^2 \Delta^2}}, \quad p_f = \sqrt{2\mu m} \quad (29)$$

The domain between the Fermi surfaces contributes to the magnetization M in Eq.(26), but it is cut out from the domain of integration in the gap equation Eq.(27). When the magnetization increases, the domain of integration in the gap equation decreases. Near the quantum critical point the size of the gap is small, and hence the linearized gap equation can be considered. Then it is easy to obtain the critical value of the magnetization M_{SC} [15]

When the magnetization approaches zero, the domain between the Fermi surfaces decreases. One can approximate the equation for magnetization Eq.(26) substituting p_f^\pm from Eq.(29) in the the difference $(p_f^+)^2 - (p_f^-)^2$ and setting $p_f^\pm = p_f$ elsewhere. Then, in this approximation, the magnetization is linear in Δ , namely

$$\Delta = \sqrt{\frac{\pi}{3}} J \kappa M \quad (30)$$

where κ runs the interval $(0, 1)$, and satisfies the equation

$$\kappa \sqrt{1 - \kappa^2} + \arcsin \kappa = \frac{8\pi^2}{m p_f J} \quad (31)$$

The Eq.(31) has a solution if $m p_f J > 16\pi$. Substituting M from Eq.(30) in Eq.(27), one arrives at an equation for the gap. This equation can be solved in a standard way and the solution is

$$\Delta = \sqrt{\frac{16\pi}{3} \frac{\Lambda p_f \kappa}{m}} \exp \left[-\frac{3}{2} I(\kappa) - \frac{24\pi^2}{J^2 V_1 m p_f} \right] \quad (32)$$

$$I(\kappa) = \int_{-1}^1 dt t^2 \ln \left(1 + \sqrt{1 - \kappa^2 t^2} \right)$$

Eqs (30,31,32) are the solution of the system Eqs.(26,27) near the quantum transition to paramagnetism.

One can write the momentum distribution functions $n^\uparrow(p, t)$ and $n^\downarrow(p, t)$ of the spin-up and spin-down quasi-particles in terms of the distribution functions of the Bogoliubov fermions

$$n^\uparrow(p, t) = u^2(p, t) n_1(p, t) + v^2(p, t) n_2(p, t) \quad (33)$$

$$n^\downarrow(p, t) = u^2(p, t) (1 - n_1(p, t)) + v^2(p, t) (1 - n_2(p, t))$$

where $u(p, t)$ and $v(p, t)$ are the coefficients in the Bogoliubov transformation. At zero temperature $n_1(p, t) = 1$, $n_2(p, t) = \Theta(-E_2(p, t))$, and the Fermi surfaces Eq.(29) manifest themselves both in the spin-up and spin-down momentum distribution functions. The functions are depicted in Fig.1 and Fig.2.

The two Fermi surfaces explain the mechanism of Cooper pairing. In the ferromagnetic phase n^\uparrow and n^\downarrow have different (majority and minority) Fermi surfaces (see Fig.3 and Fig.4, $t = 0$ graphs). The spin-up electrons contribute the majority Fermi surface, and spin-down electrons contribute the minority Fermi surface. When the value of the momentum of the emitted or absorbed magnon lies within interval $(p_f - \Lambda, p_f + \Lambda)$ the effective potential between spin-up and spin-down electrons is attracting. Hence, if the Fermi momenta p_f^\uparrow and p_f^\downarrow lie within interval $(p_f - \Lambda, p_f + \Lambda)$ the interaction between spin-up electrons, which contribute the majority Fermi surface, and spin-down electrons, which contribute the minority Fermi surface, is attracting. As a result, spin-up electrons from majority Fermi surface transfer

to the minority Fermi surface and form spin anti-parallel Cooper pairs, while spin-down electrons from minority Fermi surface transfer to the majority one and form spin anti-parallel Cooper pairs too. As a result, the onset of superconductivity is accompanied by the appearance of a second Fermi surface in each of the spin-up and spin-down momentum distribution functions (see Fig.3 and Fig.4, $t = 1$ graphs).

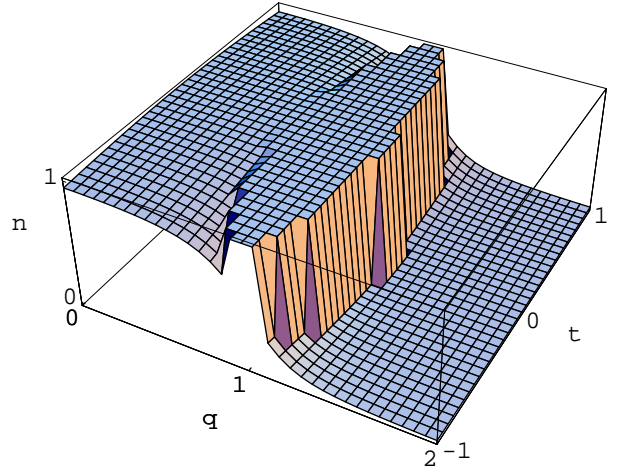


FIG. 1. The zero temperature momentum distribution n , for spin up fermions, as a function of $q = \frac{p}{p_f}$ and $t = \cos \theta$.

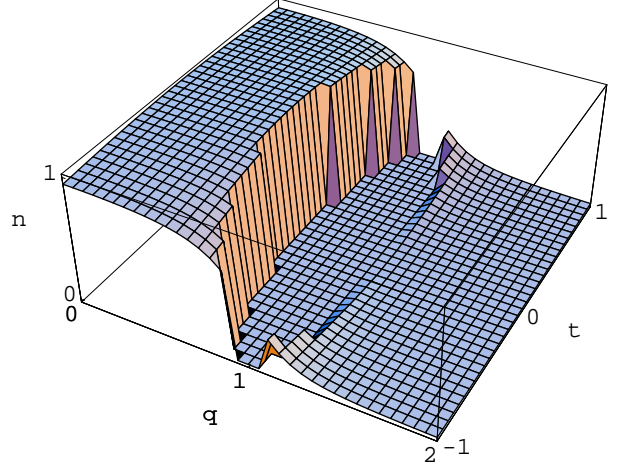


FIG. 2. The zero temperature momentum distribution n , for spin down fermions, as a function of $q = \frac{p}{p_f}$ and $t = \cos \theta$.

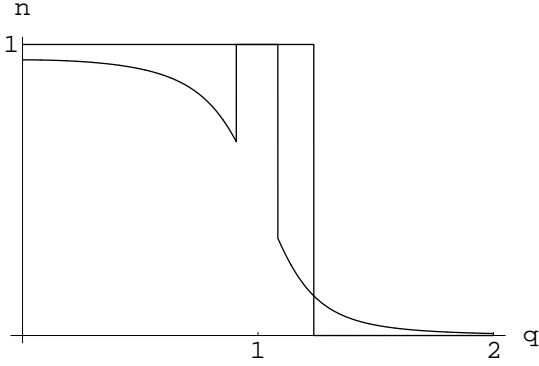


FIG. 3. The zero temperature momentum distribution n , for spin up fermions, as a function of $q = \frac{p}{p_f}$ for $t = 0$ (the gap is zero) and $t = \pm 1$ (the gap is maximal).

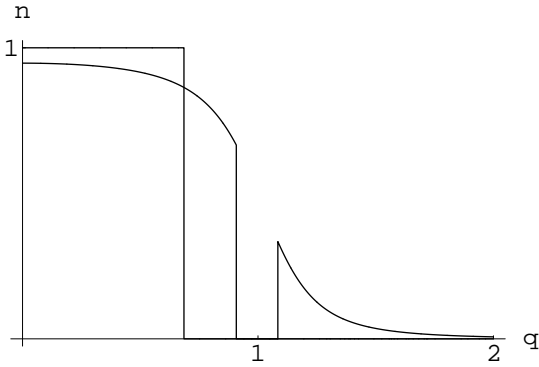


FIG. 4. The zero temperature momentum distribution n , for spin down fermions, as a function of $q = \frac{p}{p_f}$ for $t = 0$ (the gap is zero) and $t = \pm 1$ (the gap is maximal).

The existence of the two Fermi surfaces explains the linear dependence of the specific heat at low temperatures:

$$\frac{C}{T} = \frac{2\pi^2}{3} (N^+(0) + N^-(0)) \quad (34)$$

Here $N^\pm(0)$ are the density of states on the Fermi surfaces. One can rewrite the $\gamma = \frac{C}{T}$ constant in terms of Elliptic Integral of the second kind $E(\alpha, x)$

$$\gamma = \frac{mp_f}{3\kappa} \left[(1+s)^{\frac{1}{2}} E\left(\frac{1}{2} \arcsin \kappa, \frac{2s}{s+1}\right) + (1-s)^{\frac{1}{2}} E\left(\frac{1}{2} \arcsin \kappa, \frac{2s}{s-1}\right) \right]. \quad (35)$$

where $s = \frac{JMm}{p_f^2} < 1$ and $\kappa = \sqrt{\frac{3}{\pi} \frac{\Delta}{JM}}$. The Eq.(35) shows that in the ferromagnetic phase ($\Delta = 0$) the specific heat constant γ is smaller than in the superconducting one, which closely matches the experiments with UGe_2 .

III.2 Solution which satisfies $\sqrt{\frac{3}{\pi}}\Delta > JM$

In the present sub-chapter one looks for a solution of the system which satisfies

$$\sqrt{\frac{3}{\pi}}\Delta > JM \quad (36)$$

The inequality Eq.(36) shows that the gap can not be arbitrarily small when the magnetization is finite. Hence the system undergoes the quantum phase transition from ferromagnetism to FM-superconductivity with a jump. Approaching the quantum critical point from the ferromagnetic side, one sets the gap equal to zero in the equation for the magnetization (26) and considers the gap equation (27) with magnetization as a parameter. It is more convenient to consider the free energy as a function of the gap for the different values of the parameter M . To this purpose I introduce the dimensionless "gap" x and the parameters s, λ and g

$$x = \sqrt{\frac{3}{\pi}} \frac{m}{p_f^2} \Delta, \quad s = \frac{m}{p_f^2} JM, \quad \lambda = \frac{\Lambda}{p_f}, \quad g = \frac{J^2 V_1 m p_f}{8\pi^2} \quad (37)$$

Then the free energy is a function of x and depends on the parameters s, λ and g .

$$F(x) = \frac{6m^2}{\pi p_f^4} (\mathcal{F}(x) - \mathcal{F}(0)) = x^2 + g \int_{-1}^{1+\lambda} dq q^2 \int_{-1}^1 dt \times \left[\left(s - \sqrt{(q^2 - 1)^2 + t^2 x^2} \right) \Theta(\sqrt{(q^2 - 1)^2 + t^2 x^2} - s) - \left(s - \sqrt{(q^2 - 1)^2} \right) \Theta(\sqrt{(q^2 - 1)^2} - s) \right] \quad (38)$$

The dimensionless free energy $F(x)$ is depicted in Fig.5 for $\lambda = 0.08, g = 20$ and three values of the parameter $s, s = 0.8, s = 0.69$ and $s_{cr} = 0.595$. As the graph shows, for some values of the microscopic parameters λ and g , and decreasing the parameter s (the magnetization), the system passes through a first order quantum phase transition. The critical values s_{cr} and x_{cr} satisfy $\frac{x_{cr}}{s_{cr}} = \sqrt{\frac{3}{\pi}} \frac{\Delta_{cr}}{JM_{cr}} > 1$ in agreement with Eq.(36).

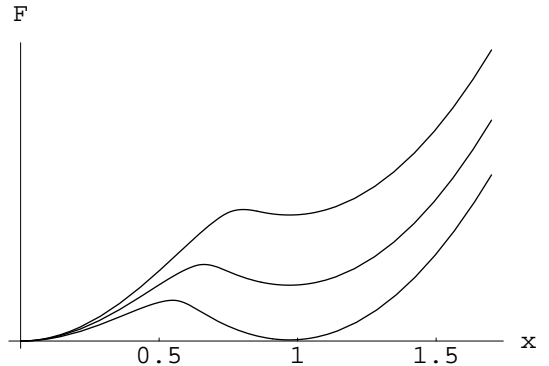


FIG. 5. The dimensionless free energy $F(x)$ as a function of dimensionless gap x . $\lambda = 0.08, g = 20, s_1 = 0.8$ (upper line), $s_2 = 0.69$ (middle line) and $s_{cr} = 0.595$ (lower line).

Varying the microscopic parameters beyond the critical values, one has to solve the system of equations (26,27). One represents again the gap in the form

$$\Delta = \sqrt{\frac{\pi}{3}} \kappa(M) J M \quad (39)$$

but now $\kappa(M) > 1$. Then the equation $E_2(k, t) = 0$, which defines the Fermi surface, has no solution if $-1 < t < -\frac{1}{\kappa(M)}$ and $\frac{1}{\kappa(M)} < t < 1$, and has two solutions

$$p_f^\pm = \sqrt{p_f^2 \pm m \sqrt{J^2 M^2 - \frac{3}{\pi} t^2 \Delta^2}} \quad (40)$$

when $-\frac{1}{\kappa(M)} < t < \frac{1}{\kappa(M)}$.

The solutions (40) determine the two pieces of the Fermi surface. They stick together at $t = \pm \frac{1}{\kappa(M)}$, so that the Fermi surface is simple connected. The domain between pieces contributes to the magnetization M in Eq.(26), but it is cut out from the domain of integration in the gap equation Eq.(27). The Fermi surface manifests itself both in the spin-up and spin-down momentum distribution functions. The functions are depicted in Fig.6 and Fig.7.

When the magnetization approaches zero, one can approximate the equation for magnetization Eq.(26) substituting p_f^\pm from Eq.(40) in the the difference $(p_f^+)^2 - (p_f^-)^2$ and setting $p_f^\pm = p_f$ elsewhere. Then, in this approximation, the magnetization is linear in Δ , namely

$$\Delta = \sqrt{\frac{\pi}{3}} J \kappa M \quad (41)$$

where $\kappa = \frac{m p_f J}{16\pi}$ is the small magnetization limit of $\kappa(M)$. The Eq.(41) is a solution if $m p_f J > 16\pi$ (see Eq.(36)). Substituting M from Eq.(41) in Eq.(27), one arrives at an equation for the gap. This equation can be solved in a standard way and the solution is

$$\Delta = \sqrt{\frac{16\pi}{3}} \frac{p_f \Delta}{m} \exp \left[-\frac{24\pi^2}{m p_f J^2 V_1} - \frac{\pi}{4\kappa^3} + \frac{1}{3} \right] \quad (42)$$

Eqs (41,42) are the solution of the system near the quantum transition to paramagnetism. The second derivative of the free energy Eq.(38) with respect to the gap is positive when $\frac{m p_f J}{16\pi} > \left(\frac{21\pi}{16}\right)^{\frac{1}{3}}$, hence the state where the superconductivity and the ferromagnetism coexist is stable.

The existence of the Fermi surface explains the linear dependence of the specific heat at low temperature:

$$\frac{C}{T} = \frac{2\pi^2}{3} N(0) \quad (43)$$

Here $N(0)$ is the density of states on the Fermi surface. One can rewrite the $\gamma = \frac{C}{T}$ constant in terms of Elliptic Integral of the second kind $E(\alpha, x)$

$$\gamma = \frac{m p_f}{3\kappa(M)} \left[(1+s)^{\frac{1}{2}} E\left(\frac{\pi}{4}, \frac{2s}{s+1}\right) + (1-s)^{\frac{1}{2}} E\left(\frac{\pi}{4}, \frac{2s}{s-1}\right) \right]. \quad (44)$$

where $s < 1$ (see Eq.(37)).

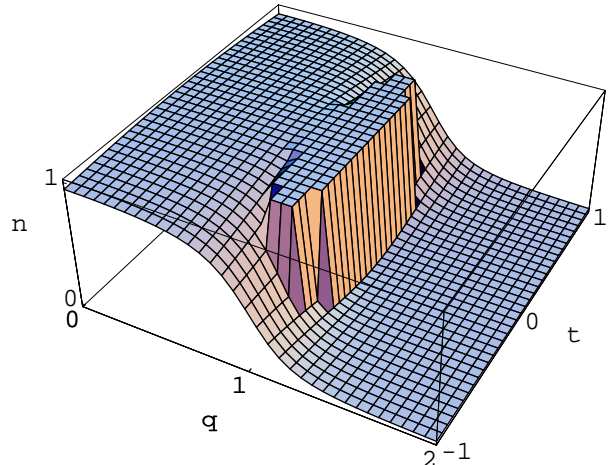


FIG. 6. The zero temperature momentum distribution n , for spin up fermions, as a function of $q = \frac{p}{p_f}$ and $t = \cos \theta$.

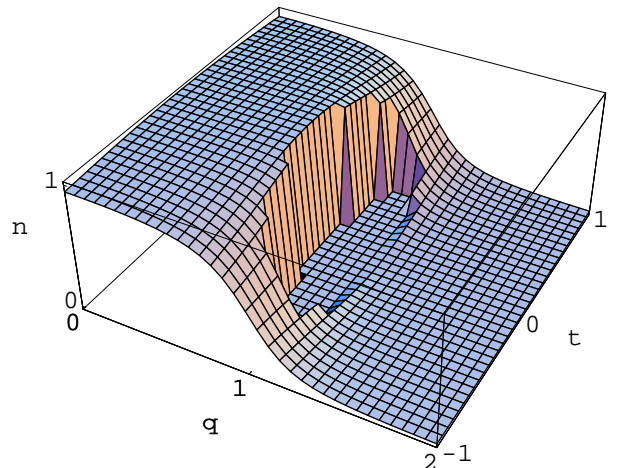


FIG. 7. The zero temperature momentum distribution n , for spin down fermions, as a function of $q = \frac{p}{p_f}$ and $t = \cos \theta$.

Eq.(44) shows that for $\kappa(M)$ just above one the specific heat constant γ is smaller in ferromagnetic phase, while for $\kappa(M) \gg 1$ it is smaller in FM-superconducting phase. The result closely matches the experiments with $ZrZn_2$ and $URhGe$ respectively.

The solutions Eqs.(30,41) show that magnetization and superconductivity disappear simultaneously. It results from the equation of magnetization, which in turn is added to ensure that the fermions which form Cooper pairs are the same as those responsible for spontaneous

magnetization. Hence, the fundamental assumption that superconductivity and ferromagnetism are caused by the same electrons leads to the experimentally observable fact that the quantum phase transition is a transition to paramagnetic phase without superconductivity.

An important experimental fact is that $ZrZn_2$ and $URhGe$ are superconductors at ambient pressure as opposed to the existence of a quantum phase transition in UGe_2 . To comprehend this difference one considers the potential (25). The quantum phase transition results from the existence of a momentum cutoff Λ , above which the potential is repulsive. In turn, the cutoff existence follows from the relation $\beta = \frac{\rho}{2Mb} > 1$, which is true when the spin-wave approximation expression for the spin stiffness constant $\rho = M\rho_0$ is used. The spin wave approximation correctly describes systems with a large magnetization, for example UGe_2 . But in order to study systems with small magnetization, one has to account for the magnon-magnon interaction which changes the small magnetization asymptotic of ρ , $\rho = M^{1+\alpha}\rho_0$, where $\alpha > 0$. Then for a small M $\beta < 1$, and the potential is attractive for all momenta. Hence for systems which, at ambient pressure, are close to quantum critical point, as $ZrZn_2$ and $URhGe$, the magnon self-interaction renormalizes the spin fluctuations parameters so that the magnons dominate the pair formation and quantum phase transition can not be observed. But if one applies an external magnetic field, the magnon opens a gap proportional to the magnetic field. Increasing the magnetic field the paramagnon domination leads to first order quantum phase transition.

IV Conclusions

The proposed model of ferromagnetic superconductivity differs from the models discussed in [7,8,9,10] in many aspects. First, the superconductivity is due to the exchange of magnons, and the model describes in an unified way the superconductivity in UGe_2 , $ZrZn_2$ and $URhGe$. Second, the paramagnons have pair-breaking effect. So, the understanding the mechanism of paramagnon suppression is crucial in the search for the ferromagnetic superconductivity with higher critical temperature. For example, one can build such a bilayer compound that the spins in the two layers are oriented in two non-collinear directions, and the net ferromagnetic moment is nonzero. The paramagnon in this phase is totally suppressed and the low lying excitations consist of magnons and additional spin wave modes with linear dispersion $\epsilon(k) \sim k$ [19]. If the new spin-waves are pair breaking, their effect is weaker than those of the paramagnons, and hence the superconducting critical temperature should be higher. Third, the order parameter is a spin antiparallel component of a spin triplet with zero spin projection. The existence of two Fermi surfaces in each of the spin-up and spin-down momentum distribution functions leads to a linear temperature dependence of the specific heat

at low temperature.

The proposed model of magnon-induced superconductivity does not contain the relativistic effects, namely spin-orbital coupling which is present in UGe_2 . The resulting magneto-crystalline anisotropy will modify the spin-wave excitation and will add a gap in the magnon spectrum, which changes the potential Eq.(25). The physical consequence of the change is that the superconductivity disappears before the quantum phase transition from ferromagnetism to paramagnetism (see [6,14]). The distance between these two points depends on the anisotropy.

ACKNOWLEDGMENTS

The author would like to thank C. Pfleiderer for valuable discussions.

-
- * Electronic address: naoum@phys.uni-sofia.bg
- [1] S. Saxena, P. Agarwal, K. Ahilan, F. M. Grosche, R. Haselwimmer, M. Steiner, E. Pugh, I. Walker, S. Julian, P. Monthoux, G. Lonzarich, A. Huxley, I. Sheikin, D. Braithwaite, and J. Flouquet, Nature (London) **406**, 587 (2000).
 - [2] C. Pfleiderer, M. Uhlarz, S. Hayden, R. Vollmer, H.v. Löhneysen, N. Bernhoeft, and G. Lonzarich, Nature (London) **412**, 58 (2001).
 - [3] D. Aoki, A. Huxley, E. Ressouche, D. Braithwaite, J. Flouquet, J-P. Brison, E.Lhotel, and C. Paulsen, Nature (London) **413**, 613 (2001).
 - [4] A. Huxley, I. Sheikin, E. Ressouche, N. Kernavanois, D. Braithwaite, R. Calemczuk, and J. Flouquet, Phys. Rev. B **63**, 144519 (2001).
 - [5] C. Pfleiderer and A.Huxley, arXiv: cond-mat/0208115 (2002).
 - [6] N. Tateiva, T. Kobayashi, K. Hanazono, K. Amaya, Y. Haga, R. Settai, and Y. Onuki, J. Phys. Condens. Matter **13**, L17 (2001).
 - [7] C. P. Enz, and P. T. Matthias, Science **201**, 828 (1978).
 - [8] D. Fay, and J. Appel, Pys.Rev. B **22**, 3173 (1980).
 - [9] T. Kirkpatrick, D. Belitz, T. Vojta and R. Narayanan Phys. Rev. Lett. **87**, 127003 (2001).
 - [10] M. B. Walker, and K. V. Samokhin, Phys. Rev. Lett. **88**, 207001 (2002).
 - [11] K. Machida, and T. Ohmi, Phys. Rev. Lett.**86**, 850 (2001).
 - [12] R. Roussev and A.Millis, Phys. Rev. B **63**, 140504 (2001).
 - [13] Z. Wang, W. Mao, and K. Bedell, Phys. Rev. Lett. **87**, 257001 (2001).
 - [14] E. Bauer, et al., J. Phys. Condens. Matter **13** L759 (2001).
 - [15] N. Karchev, arXiv: cond-mat/0206534 (2002)
 - [16] N. Karchev, K. Blagoev, K. Bedell, and P. Littlewood, Phys. Rev. Lett., **86** 846 (2001).

- [17] N. F. Berk, and J. R. Schrieffer, *Phys. Rev. Lett.* **17**, 433 (1966).
- [18] J. W. Negele and H. Orlando, *Quantum Many-Particle Systems* (Addison-Wesley, 1988)
- [19] S. Sachdev, and T. Senthila, *Ann.Phys.(NY)* **251**, 76 (1996)